INTERFACE SCIENCE IN THERMAL BARRIER COATINGS

Failure mechanisms of thermal barrier coatings on MCrAlY-type bondcoats associated with the formation of the thermally grown oxide

**Dmitry Naumenko · Vladimir Shemet ·
Lorenz Singheiser · Willem Josef Quadakkers**

Abstract The effect of the thermally grown oxide (TGO) formation on the lifetime of the thermal barrier coatings (TBC) with MCrAlY-bondcoats (BC) is reviewed. A number of factors affecting the TGO-formation and TBC-failure are discussed including the coating microstructure, geometrical (coating roughness and thickness) and processing parameters. Under given testing conditions for a specific EB-PVD-TBC-system forming a flat, uniform alumina TGO a critical TGO-thickness for TBC-failure can be defined. This TGO-morphology is, however, not necessarily optimum for obtaining long TBC-lifetime, which can be extended by formation of TGO's with an uneven TGO/BC interface. In contrast, APS-TBC-systems are prone to formation of intrinsically inhomogeneous TGO-morphologies. This is attributed to non-uniform depletion of Y and Al underneath rough MCrAlY-surfaces as well as due to the commonly observed repeated-cracking/re-growth of the TGO during temperature cycling. The latter phenomenon depends on the exposure temperature and the mechanical properties of the APS-TBC. In both types of TBC-systems the TGO-formation and TBC-lifetime appear to be very sensitive to the manufacturing parameters, such as vacuum quality during bondcoat spraying and temperature regime of the bondcoat vacuum heat-treatment.

Introduction

The demand for improved efficiencies in energy conversion systems has in the recent years led to the introduction of gas turbines with significantly increased gas inlet temperatures.

D. Naumenko (✉) · V. Shemet · L. Singheiser ·
W. J. Quadakkers
Forschungszentrum Jülich GmbH, IEF-2, 52425 Juelich,
Germany
e-mail: d.naumenko@fz-juelich.de

Handling of such high temperatures requires the use of high strength directionally solidified and single crystalline Ni-base superalloys. In addition, the components of the hottest sections are internally cooled and protected by ceramic thermal barrier coatings (TBCs), which allow component operation at gas temperatures in the range of the melting point of the superalloy. The TBC coatings, mostly consisting of yttria stabilized zirconia, are commonly applied on the structural components by electron beam assisted vapor deposition (EB-PVD) or air plasma spraying (APS). A metallic bond coat (BC) between the zirconia-based TBC and the nickel-base alloy provides oxidation resistance for the base material and is responsible for adherence of the ceramic coating [1, 2]. Depending on the actual operating conditions TBC life can be affected by a number of factors, however, nearly all researchers consider bond coat (BC) oxidation to be a crucial parameter for TBC life [3, 4].

In the present article, the oxidation of MCrAlY-bond-coats (M = Ni, Co) and its effect on the lifetime of TBC's will be discussed based on literature data as well as authors' own experimental results. First, the TBC-failure associated with the TGO-formation will be considered for EB-PVD and APS-TBC's. Then, the effect of various parameters related to MCrAlY-bondcoat oxidation on TBC-lifetime will be elucidated. The latter will include the phase composition and microstructure, geometrical and manufacturing parameters of the MCrAlY-coatings.

TBC-failure and defect formation in/near TGO

General remarks

Although nearly all researchers agree on the significance of bond coat oxidation for TBC life, the exact failure

Fig. 1 **a** Relative lifetime data (multiple specimens) of APS-TBC-system with NiCoCrAlY-bondcoat on Ni-base superalloy as a function of temperature in cyclic oxidation test (2 h heating/15 min cooling) in air and **b** Effect of cycling parameters on lifetime at 1,050 °C
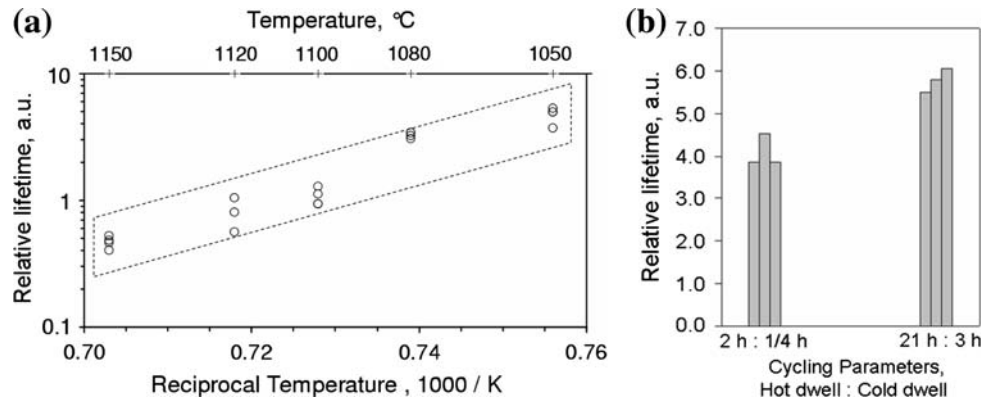
mechanisms for the various coating types are not completely clarified. In some cases the TBC-failure was associated with the Al-depletion in the bondcoat resulting in the formation of large amounts of Ni,Cr-rich spinel oxides [5]. In most of the cases, however, the TBC fails prior to the occurrence of critical Al-depletion required for spinel formation. The time to failure depends on the cycle frequency and oxidation temperature (Fig. 1), whereby quite often the values exhibit considerable scatter even for a single coating system [6]. For proprietary reasons the TBC-lifetimes in Fig. 1 and in other figures in the present article are given as relative values in arbitrary units (a.u.). These relative lifetimes were calculated by dividing the measured TBC-lifetimes in hours at high temperature by a constant.

The failure of EB-PVD-TBC coatings in service is claimed to occur by spallation of the thermally grown oxide (TGO) or in some cases by crack formation in the TGO, whereas in APS-TBC's the failure seems to occur within the TBC in the vicinity of the TGO [3]. APS-coated systems therefore frequently show the so-called white failure, i.e., after spallation significant parts of the ceramic remain adherent to the bond coat (Fig. 2b). In the following the mechanisms of defect formation in the TGO and failure of the EB-PVD and APS-TBCs will be discussed in more detail.

Failure of EB-PVD-TBC's on MCrAlY-bondcoats

The commonly accepted failure mechanism of EB-PVD TBCs with MCrAlY-bondcoats is crack initiation and propagation at the TGO/bondcoat interface followed by macroscopic buckling and spallation of the TBC. This failure mechanism is different from that observed by several authors [3, 7] in EB-PVD-TBC with (Ni,Pt)Al-bondcoats, which can fail by rumpling of the TGO, whereby the TBC fails at the TBC/TGO-interface.

For flat interfaces the mechanisms of oxide scale delamination from the metal substrate were categorized by Evans [8] into buckling and wedging. The buckling mechanism predominates for compact scales with a small concentration of defects and relatively low interfacial toughness. Wedging is more likely to occur for thick scales with a large number of defects and a strong scale/metal interface. The latter mechanism is not considered to be important for the TBC-systems. For macroscopic TBC-buckling to occur, large delaminations are necessary, since the critical stress for buckling depends on the ratio of the TBC thickness versus delamination size [3, 8]. In reality, the TGO/BC interfaces are, in spite of smoothening of the MCrAlY-bondcoats prior to the EB-PVD-TBC deposition, not ideally flat. They thus provide nucleation sites for crack initiation. Consequently, the critical stage for the lifetime of an EB-PVD-TBC is the crack growth at the scale/metal interface, rather than crack nucleation. For an EB-PVD-TBC-system with a Pt-coated MCrAlY-bondcoat it was shown [9] that the crack growth during cyclic oxidation at 1,000 °C can be a relatively slow process proceeding during several thousands of hours exposure. At some point, however, linking of the cracks occurs, which leads to a rapid crack propagation and subsequent macroscopic

Fig. 2 Examples of macroscopic failure appearances of **a** EB-PVD and **b** APS-TBC coatings after long-term cyclic air oxidation at 1,050 °C
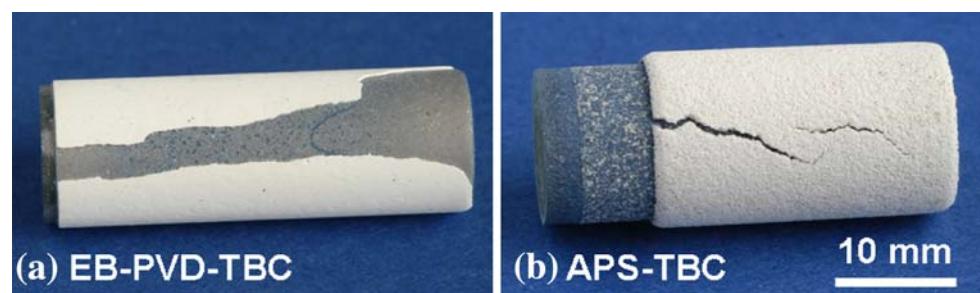
TBC-failure by buckling. The rate of crack propagation at the TGO/BC interface depends strongly on the interfacial toughness [3]. For MCrAlY model alloys and coatings without TBC the latter parameter was shown to be adversely affected by the sulfur content in the coating and the substrate as well as by the presence of water vapor in the test atmosphere [10].

The driving force for crack initiation and propagation at the TGO/BC interface is the elastic strain energy accumulated in the TGO (and TBC) during cooling due to mismatch with the metal substrate. It has been suggested [8] that for a given coefficient of thermal expansion (CTE)-mismatch and temperature drop a critical oxide scale thickness for delamination exists, which corresponds to the critical strain energy. This means that higher TGO-growth rates should result in shorter TBC-lifetime.

Using the critical scale thickness approach, optimization of the oxidation behavior of MCrAlY alloys and coatings until recently has aimed at minimization of the alumina scale growth rates [11]. In a number of studies, however, it has been shown that the time to TBC-failure cannot be straightforwardly correlated with a certain oxide scale thickness valid for all systems with MCrAlY-bondcoats. It was observed that the TGOs containing physical defects (micro-pores), with an increased amount of reactive element (RE) oxide pegs [12, 13] are capable of maintaining good TGO and TBC adherence in spite of enhanced growth rate compared to thin, defect free scales [14]. Figure 3 shows SEM-images of two TBC-systems with NiCoCrAl-Y-bondcoats, whereby one of the bondcoats had a minor addition of Zr. The Zr-free bondcoat forms a thin, uniform TGO. In contrast, the Zr-containing bondcoat forms a non-uniform TGO with a number of cracks in its outer part near the interface to the TBC. The effect of Zr on accelerating the alumina scale growth rate is similar to that known to occur in other alloy systems, such as wrought FeCrAlY + Zr alloys [15]. It is related to ZrO_2 incorporation into the growing alumina scale, thus providing short-circuit paths for inward oxygen transport. Surprisingly, the lifetime of the TBC-system with the more rapidly oxidizing, Zr-containing bondcoat is by approximately a factor of two longer than that with the Zr-free bondcoat.

This TBC-lifetime extension with the Zr-doped bondcoat is related to the specific non-uniform scale morphology, which impedes the crack propagation at the TGO/bondcoat interface. Similar effects on the TGO-morphology were observed to be caused by the presence of Hf in the MCrAlY-bondcoat, either as intentionally added element (reference [16] and Fig. 23 in the present article) or by Hf incorporation as a result of diffusion from the substrate superalloy [13]. In the latter reference, Schulz et al. showed that incorporation of Hf diffusing from single crystal superalloys improves TGO-adherence by formation of Hf-rich oxide pegs at the scale/metal interface resulting in extended TBC-lifetime compared to Hf-free superalloys. An additional effect of Hf on the improved TGO-adherence can be associated with gettering coating/alloy impurities such as sulfur and carbon [11]. It is important to note that the positive effect of Hf and/or Zr on the TGO-morphology and associated TBC-lifetime crucially depends on the distribution of these reactive elements (REs) in the coating. This distribution is in turn strongly affected by the manufacturing parameters of the MCrAlY-coatings, such as the vacuum quality during VPS-spraying and the temperature

Fig. 3 a Results of lifetime cyclic oxidation testing (at 1,050 °C in air; each cycle: 2 h heating, 15 min cooling) of EB-PVD-TBC-systems with NiCoCrAlY-bondcoats with and without minor Zr addition; SEM cross-sections after 100 h exposure of TBC specimens b BC without Zr, and c with Zr
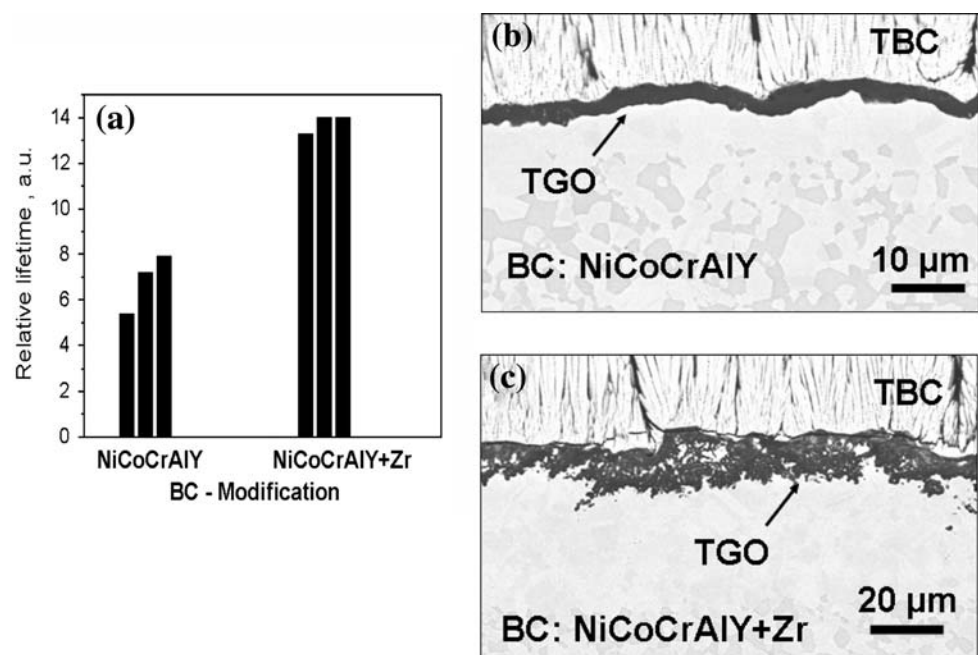
regime during heat-treatment. These issues are discussed in detail in the sections "Effect of manufacturing related parameters on MCrAlY-oxidation behavior and TBC-lifetime" and "Effect of heat-treatment parameters on RE-distribution and TGO-growth" later on in the present article.

Failure mechanisms of APS-TBC's on MCrAlY-bondcoats

Figure 4 shows an example of failure for an APS-TBC-system after long-term cyclic oxidation at 1,100 °C. On large parts of the specimen, remnants of the TBC are still
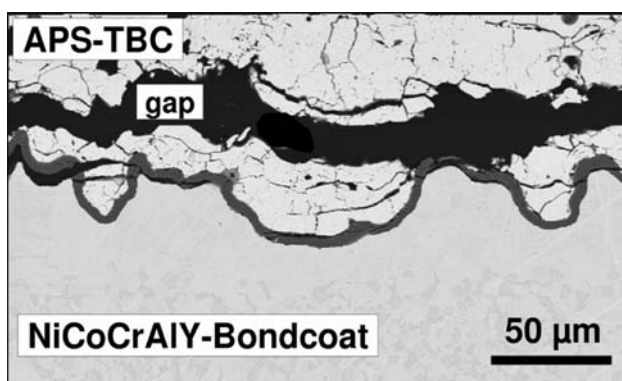

Fig. 4 Cross-section showing typical failure of APS-TBCs on MCrAlY-bondcoat after cyclic oxidation at 1,100 °C in air
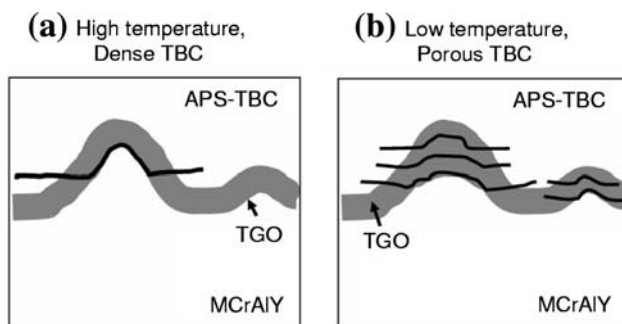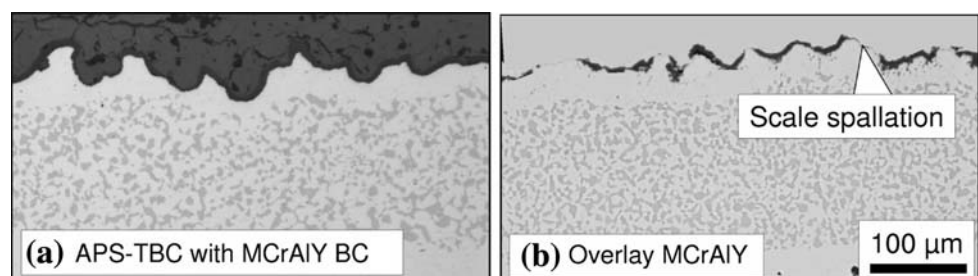

Fig. 5 Schematic illustrating different crack propagation modes in APS-TBC-systems

adhering to the BC and the main crack seems to be present in the inner part of the TBC. In the failure interpretation it has, however, to be considered that the bondcoat used for APS-TBC's has a high surface roughness. The result in Fig. 4 indicates a failure mechanism as illustrated schematically in Fig. 5a. During cooling, high compressive stresses occur in the TGO in the valleys of the rough bondcoat surface, which do not lead to spallation. On the hills of the rough surface, however, the geometry imposes generation of tensile out-of-plane stresses in the TGO upon cooling [17]. These tensile out-of-plane stresses lead to crack initiation at the TGO/BC interface. The resistance of the interface to delamination depends on the interfacial toughness (TGO-adhesion) as well as the TGO-thickness and the radius of curvature; the latter two parameters determining the magnitude of the stress. The crack initially propagates along the TGO/BC interface at the hill following the roughness profile. Propagating toward the valley the interfacial out-of-plane tensile stress decreases and, simultaneously, the in-plane shear stress increases. At some point after reaching a critical shear stress fracture of the alumina scale occurs and the crack penetrates the TGO and subsequently the TBC. In the TBC the crack propagates approximately parallel to the BC/TBC interface thereby leaving the TBC and the TGO in the valleys unaffected. These results imply that in the case of APS-TBC-systems the exact definition and reproducible manufacturing of an optimum bond coat surface roughness profile is of great importance for obtaining a reproducible TBC life.

It should be noted that first delamination of the TGO at the BC-hills occurs after relatively short times compared to the times to macroscopic TBC-failure. This is apparent from the metallographic images in Fig. 6a, which show that in the case of the NiCoCrAlY-bondcoat without the TBC considerable scale spallation from the hills was found already after 1,000 h at 1,000 °C. In contrast, in the TBC-system the delaminated parts of the scale in the hills are constrained by the TBC (Fig. 6b).

The rate of crack propagation depends on the temperature cycling conditions, but also on the microstructure of the TGO and TBC (porosity, grain size, etc.). For example, porosity in the TBC reduces its apparent elastic modulus,

Fig. 6 Metallographic cross-sections of Ni-base superalloy coated with VPS MCrAlY after cyclic oxidation testing for 1,000 h at 1,000 °C in air: **a** with APS-TBC topcoat and **b** without APS-TBC topcoat

which should decrease the driving force (stress) for crack propagation. For many APS-TBC-systems the rate of crack propagation in the TBC is much slower than the TGO-delamination frequency in the hills. This leads to a typical TGO-morphology formed by repeated delamination cracking and re-growth in the hills (Figs. 5b and 7a).

Figure 7b shows the microstructure of the TGO after repeated-cracking and re-growth in an In-Lens SEM-image. Details of using the In-Lens SEM-technique for microstructural characterization of the alumina scales are presented in reference [18]. It is obvious that the separated TGO layers possess the columnar microstructure, which is typical for inward-growing alumina scales (compare with Figs. 12 and 13 in the section "TGO-growth rate and its effect on TBC-lifetime"). This observation excludes the possibility that the parallel cracks could have been initiated
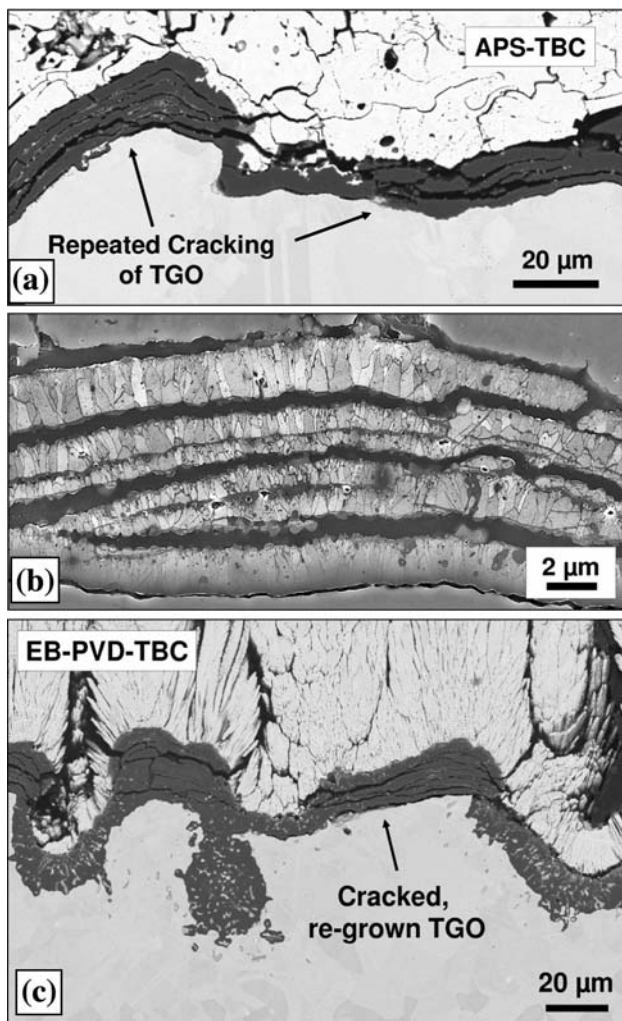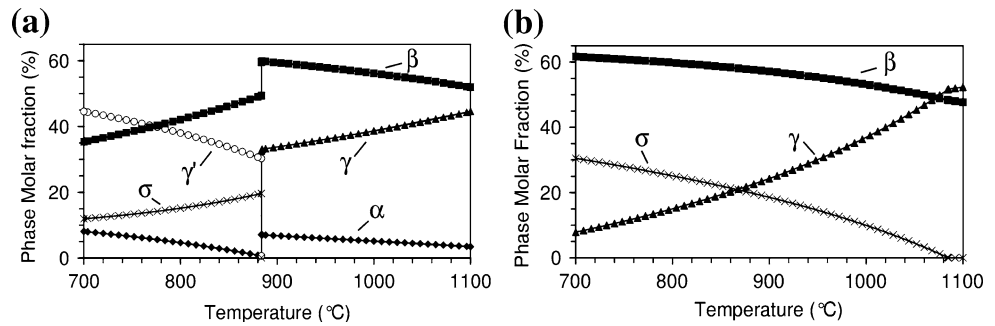

Fig. 7 Repeated TGO-cracking/re-growth during cyclic oxidation at 1,050 °C in APS-TBC-system with NiCoCrAlY-bondcoat: **a** BSE image; **b** High-resolution In-Lens SE-image and **c** EB-PVD-TBC with poorly smoothened bondcoat surface after cyclic oxidation at 1,000 °C

in the TBC and then propagated via defects in the thick alumina scale and confirms the validity of the above cracking/re-growth mechanism. Similar observations on the repeated TGO-cracking in APS-TBC-systems were also made by other authors [19, 20] and, depending on BC-roughness, can also be observed in EB-PVD-TBC-systems in the case of poor bondcoat smoothening prior to TBC deposition (Fig. 7c).

One of the reasons why the delamination cracking in the hills of the TGO/BC interface does not immediately lead to macroscopic TBC-failure becomes apparent from modeling of stress distribution in the APS-TBC-systems [21]. This modeling indicated that the crack propagation within the APS-TBC between the hills of the rough, sprayed BC-surface is only possible in the case of tensile out-of-plane stress in the TBC. This stress is expected to increase with thickening of the oxide scale, since with thin scales the calculated out-of-plane stress appeared to be compressive. In the work by Trunova et al. [22] the damage evolution in an APS-TBC-system with a NiCoCrAlY-bondcoat was assessed by considering crack formation, linking of individual cracks and crack growth. The measured maximum crack length showed a good correlation with the TGO-growth kinetics, whereas increasing the cycle frequency resulted in a decrease of the hot-time service life.

As crack propagation in the APS-TBCs depends among other factors on their microstructure and mechanical properties, the TBC-failure mechanism can vary depending on the exposure temperature, which is known to affect these properties. At high testing temperatures of approximately 1,100 °C and above, the TBC-failure tends to occur without repeated TGO-cracking/re-growth contrary to exposures at lower temperatures (compare Fig. 4 with Fig. 7). The different failure modes of the APS-TBCs are depicted schematically in Fig. 5. One of the possible explanations for the difference in the failure modes is that at higher temperatures sintering of the ceramic top-coat occurs, which increases the effective Young's Modulus thereby enhancing the effective rate of crack propagation through the TBC.

Similar to EB-PVD-TBC-systems the strain energy accumulated in the TGO beneath the APS-TBC is the driving force for crack initiation and propagation resulting finally in macroscopic TBC-failure. However, the above presented results indicate that in many cases the definition of a critical TGO-thickness for TBC-failure in APS-TBC-systems is not possible. One of the reasons is the repeated TGO-delamination and re-growth at the bondcoat hills. Another reason is the formation of an inhomogeneous TGO on rough surfaces. This phenomenon is described later in the present article (see the section "Effect of MCrAlY-coating geometrical parameters on TGO-morphology and TBC-lifetime"). On the bondcoat hills formation of rather

Fig. 8 Molar fractions of different phases in the temperature range 800–1,100 °C calculated by ThermoCalc for: **a** NiCoCrAlY + Re-coating **b** CoNiCrAlY-coating. Both coatings have approximately 20 wt% Cr and 10 wt% Al

pure alumina scales, occasionally underneath nodules of $Ni(Cr,Al)_2O_4$ spinel occurs, whereas in the valleys the scale contains Y-Al mixed oxide pegs, which locally accelerate the scale growth rate. The extent of Y and Al-depletion depends on the surface roughness and consequently the scale morphology varies along the roughness profile. Therefore, even for a particular APS-TBC-system and testing condition it is in many cases difficult to define a critical TGO-thickness for TBC-failure.

Effect of MCrAlY-coating phase transformations on TBC-lifetime

MCrAlY-coatings have nominal compositions with the alloying additions varying typically between 10–30 wt% for Co, 15–20 wt% for Cr and 8–12 wt% for Al (rest Ni) [1–4]. In addition some MCrAlY-coating compositions contain additions of refractory elements, such as Ta and/or Re in concentrations typically below 3 wt% [23, 24]. The coating microstructure prevailing at temperatures in the range of 1,050–1,100 °C typical for most laboratory exposures, consists of β-NiAl in a γ-Ni matrix. The RE, yttrium added in minor amounts to MCrAlY-alloys to improve the alumina scale adherence is mainly present in form of an intermetallic phase, such as $Ni_{17}Y_2$ due to its very low solubility in the γ and β-phases. For instance, less than 0.2 wt% Y is soluble in γ-Ni at 1,200 °C [25] and the solubility is even lower in the β–phase. In contrast, RE's such as Hf and Zr alloyed in addition to Y in some of the MCrAlY-coatings for modifying the oxidation pro, have a much higher solubility in the γ and β phases (>1wt% at 1,200 °C [25]) than Y. Consequently, at high temperatures Hf and Zr are expected to be completely dissolved in the γ-Ni matrix if present in concentrations typical for RE-additions (up to 0.6 wt% $\approx$ 0.3 at.%).

At lower temperatures in the range of 850–1,000 °C the microstructure of MCrAlY-materials can be significantly different from the two phase $\gamma+\beta$. Other phases such as γ'- Ni_3Al, σ- (Cr_XCo_Y) and α-Cr were frequently reported [26–29]. It is important to mention that the actual operating temperatures of the MCrAlY-materials in industrial gas

turbines are generally not higher than 950 °C [30]. The phase transformations in the MCrAlY-bondcoats during temperature changes can have a profound effect on the lifetime of TBCs as illustrated by the following example.

Figure 8 shows the results of Thermocalc [31] calculations using Ni-Data [32] version 7 database for two typical commercially available MCrAlY-coating compositions, a NiCoCrAlY and CoNiCrAl with similar nominal Cr and Al contents, but with a different Co/Ni ratio. In addition, the Ni-base coating had a Re-content of approximately 2 wt%.

The calculations predict a shift of the phase equilibrium from $\beta + \gamma + \alpha$ to $\beta + \gamma' + \alpha + \sigma$ to occur at around 880 °C in the Ni-base coating, which was verified by studies on free-standing, vacuum plasma sprayed (VPS) coatings [29]. The measurements of the differential CTE reveal a peak at about 850 °C (Fig. 9). This peak indicates that the γ to γ' transformation in the NiCoCrAlY-coating is associated with a positive volume change.

The occurrence of this transformation reaction in the NiCoCrAlY + Re-coating were confirmed by detailed analysis of the coating microstructures using a number of analytical techniques, such as scanning and transmission electron microscopy (SEM and TEM) as well as X-Ray diffraction (XRD). Figure 10a, b shows the differences in the microstructure of the NiCoCrAlY-coating between 1,100 and 800 °C.
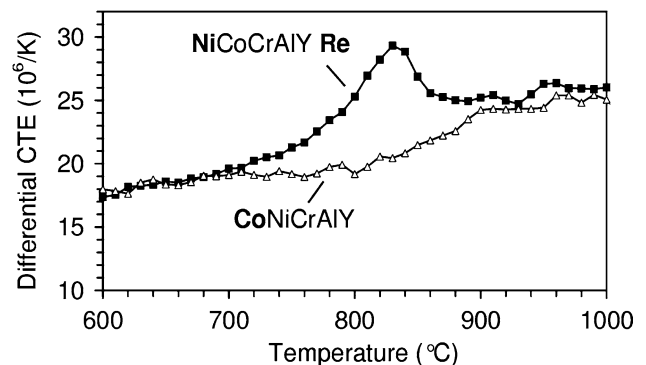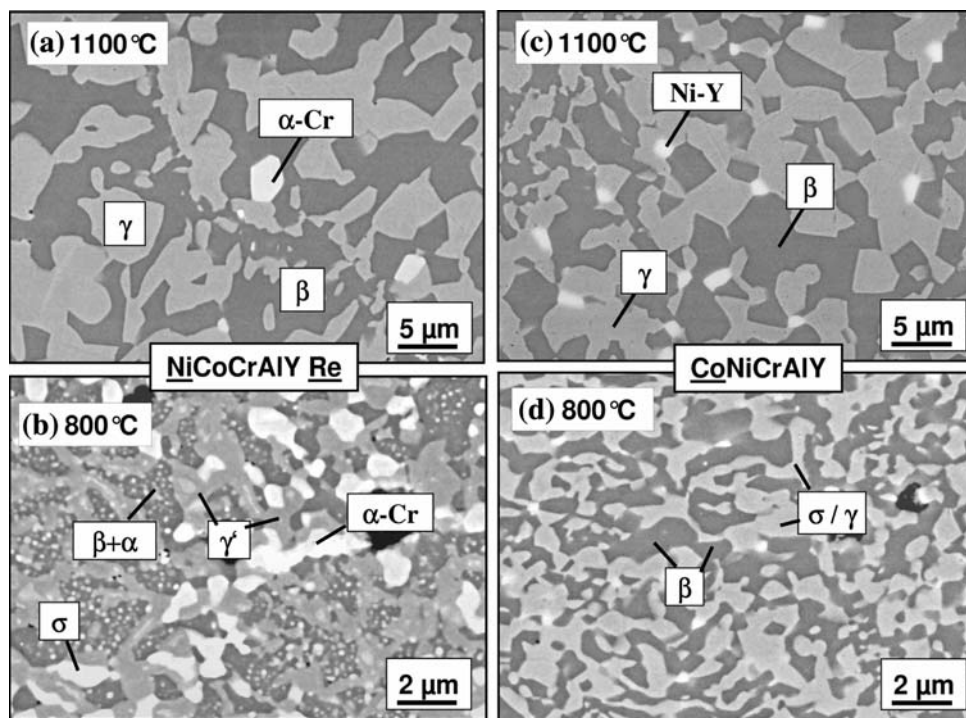
Fig. 9 Differential coefficients of thermal expansion of NiCoCrAlY + Re and CoNiCrAlY-coatings. Both coatings have approximately 20 wt% Cr and 10 wt% Al

Fig. 10 SEM-images showing microstructure of 1.5 mm thick VPS, free-standing MCrAlY-coatings after high temperature annealing at **a**, **c** 1,100 °C for 25 h and **b**, **d** 800 °C for 300 h for NiCoCrAlY + Re **a**, **b** and CoNiCrAlY **c**, **d**

The γ to γ' transformation could not be observed in the CoNiCrAlY, Re-free coating (Fig. 9, Fig. 10) in agreement with the predictions by Thermocalc (Fig. 8) and findings of other authors [28].

EB-PVD-TBC-systems with the two above-mentioned bondcoats on a Ni-base superalloy were tested in a discontinuous oxidation test with approximately 50 h cycles. The TBC-lifetime with the NiCoCrAlY-bondcoat was by almost a factor of two shorter compared to that with the CoNiCrAlY-bondcoat (Fig. 11). During cooling intervals the residual stresses in the TGO were measured using photoluminescence piezospectroscopy (PLPS, [7]). The compressive stresses in the TGO were higher in the system with the CoNiCrAlY bond coat compared to NiCoCrAlY-bondcoat (Fig. 11). Furthermore, in the TBC-system with

the CoNiCrAlY BC the stresses continuously increased with time reaching a value of approximately 6GPa at failure. In the system with the NiCoCrAlY-bondcoat, however, the residual stresses were at a constant level, slightly above 3GPa during almost all its lifetime. In contrast, the data presented in Fig. 9 indicate a slightly higher CTE for the NiCoCrAlY-bondcoat. If the deformations were purely elastic, this would result in a higher residual stress in the TGO on the NiCoCrAlY-bondcoat compared to CoNiCrAlY, i.e., opposite to the PLPS-measurements. Apparently the measured lower residual stress in the TGO with the NiCoCrAlY-bondcoat indicates a poorer TGO-adhesion. This could be a result of the above described phase transformation, which leads during cooling in a formation of a brittle matrix phase $\gamma \rightarrow \gamma'$, thereby decreasing the coating ability to relax the thermally induced stresses by creep. Consequently part of the thermal stress in the TGO on the NiCoCrAlY-bondcoat could be relaxed by oxide cracking and/or delamination resulting in a shorter time to TBC-failure with this type of bondcoat.

The results in this section indicate that the phase transformation in the MCrAlY-bondcoat can have an effect on the TBC-lifetime and should be considered when designing the bondcoat chemical compositions.
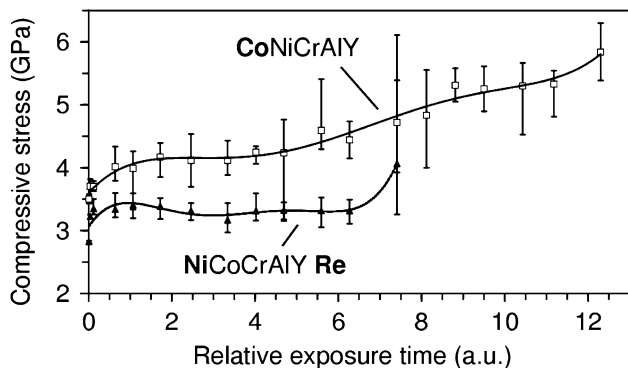

Fig. 11 TGO stresses in TBC specimens with two different bondcoat (BC) types measured during discontinuous oxidation in air at 1,100 °C till TBC-lifetime (7.5 a.u. for NiCoCrAlY + Re-BC and 12.5 a.u. for CoNiCrAlY-BC)

TGO-growth rate and its effect on TBC-lifetime

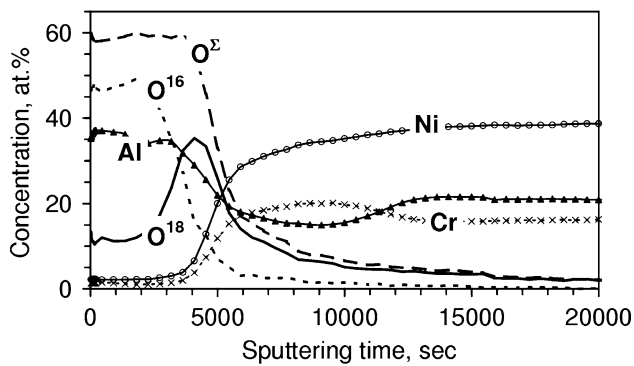The alumina scale growth rate on the MCrAlY-coatings and bondcoats was frequently observed to follow

Fig. 12 Plasma SNMS-depth profile of a 1.5 mm thick, free-standing VPS-NiCoCrAlY-coating after two-stage oxidation in Ar-20%O$_2$ at 1,100 °C for 20 h. Stage 1: 4 h in Ar − ^{16}O$_2$; Stage 2: 16 h in Ar-(^{16}O + ^{18}O)$_2$. The ^{18}O-enrichment during the second stage was 20%. Quantification into atomic percents and re-calculation to an ^{18}O-enrichment factor of 100 was performed according to the procedure described in reference [34]

Fig. 13 SEM in-lens image of TGO grown in an APS-TBC-system with a NiCoCrAlY-bondcoat after 400 h cyclic air oxidation at 1,050 °C. The nominal bondcoat composition is the same as that of the free-standing coating in Fig. 12

sub-parabolic oxidation kinetics with time exponent approaching 0.33 [33]. The reason for such a time dependence of the scale thickening is the scale growth mechanism. This is illustrated in Fig. 12, which shows an SNMS-depth profile of an alumina scale formed on a free-standing VPS NiCoCrAlY-coating after two-stage oxidation at 1,100 °C using oxygen tracers. It can be seen in Fig. 12 that the oxygen isotope present during the second oxidation stage (^{18}O) is enriched at the scale/metal interface, indicating short-circuit inward oxygen diffusion as predominant transport process in the scale. Similar observations were made with Y-oxide dispersion strengthened (ODS) FeCrAl-alloys, Y and Zr-containing β-NiAl and NiCrAl [34–36] and more recently with Y-doped wrought FeCrAl-alloys [18]. In all these studies it was claimed that the short-circuit paths for inward oxygen transport are the alumina scale grain boundaries. In reference [18] the sub-parabolic, near-cubic kinetics was quantitatively correlated with the growth mechanism and columnar microstructure of the alumina scale. The latter was shown to form by inward oxygen grain boundary diffusion combined with competitive grain growth, whereby the lateral scale grain size was found to be a linear function of the depth from the scale/gas interface. The increase in the scale grain size results in a decrease of the effective diffusion coefficient and consequently in near-cubic kinetics.

Figure 13 depicts the microstructure of the TGO in an APS-TBC-system with a NiCoCrAlY-bondcoat in an SEM, In-Lens image. A columnar grain-structure of the TGO in an APS-TBC-system can be seen. Similar observations with respect to the TGO grain-structure in an EB-PVD-system were described recently in reference [37] using EBSD. Based on the SNMS-results and SEM microstructural data (Fig. 12, Fig. 13) it can be stated that the
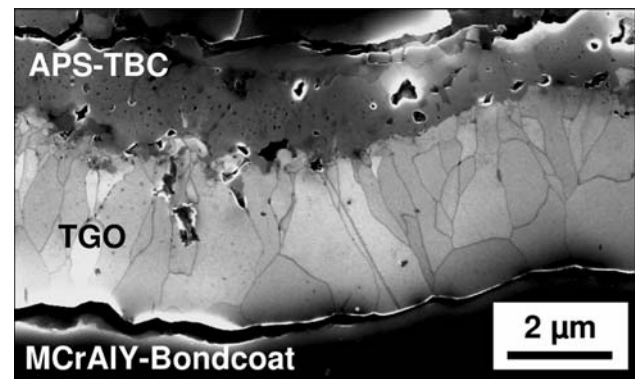
mechanism of the alumina scale formation operative in TBC-systems with NiCoCrAlY-bondcoats is similar to that described for FeCrAlY-alloys.

The oxidation rate can be influenced by temperature, RE-content in the coating and, as will be shown in the section "Effect of MCrAlY-coating geometrical parameters on TGO-morphology and TBC-lifetime", by coating thickness. However, by variation of one or more of these parameters, the TGO-morphology will be changed due to variations in the amount and distribution of yttrium-rich internal-oxide precipitates incorporated into the scale [38]. So, a variation in the TGO-thickening rate by changing (one of) the mentioned parameters will not give an unequivocal effect of TGO-thickness on the TBC-lifetime.

In order to find out how a change in the TGO-growth rate in MCrAlY-bondcoats quantitatively affects the TBC-lifetime, one should in an ideal case be able to change only the scale growth rate without changing other parameters, such as TGO-morphology and composition, temperature, mechanical properties of the bondcoat, etc. Such a variation in the TGO-growth rate is possible by exposing the TBC specimens in atmospheres in which the oxygen partial pressure considerably differs from that in air. For instance, the TGO-growth rate can be substantially reduced in low pO$_2$ environments, such as Ar-4%H$_2$-2%H$_2$O (pO$_2$ = 10^{-14} bar) [38]. The reason for such pO$_2$ dependence of the growth rate can be explained considering the described above scale growth mechanism, i.e., oxygen diffusion via oxide grain boundaries. The defect structure of the alumina scale and consequently the oxygen diffusion coefficient is practically unaffected by the change of oxygen partial pressure in the atmosphere [39]. Consequently, the reduction in the scale growth rate in H$_2$/H$_2$O-mixture is due to a reduced driving force for oxygen diffusion (oxygen chemical potential gradient). Figure 14a, b shows the TGO-morphologies after exposure in the different

Fig. 14 Cross-sections of EB-PVD-TBC specimens with NiCoCrAlY-bondcoat after cyclic oxidation at 1,100 °C in **a** air and **b** Ar-4%H_2-2%H_2O; oxidation times indicated in **c**; **c** Estimation of critical TGO-thickness by extrapolating measured TGO-thickness to TBC-failure times in air and Ar-4%H_2-2%H_2O
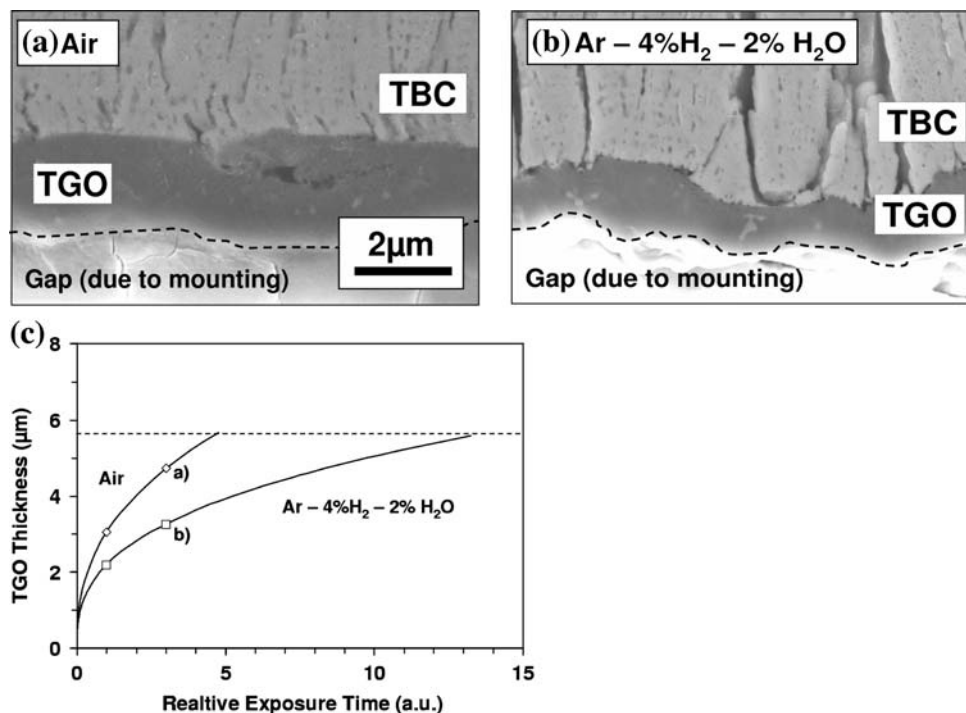
environments at 1,100 °C. The oxide scale grown on the specimen exposed in air is 5 μm thick while that formed on the specimen exposed in Ar-4%H_2-2%H_2O is only 3 μm thick. An important observation is that the oxide scales were almost identical with respect to microstructure and morphology. Subsequently, additional specimens from the same batch were exposed in the two atmospheres until TBC-failure. The lifetime of the ceramic coating was found to be by a factor of 2.5 shorter when exposed in air compared to the exposure in Ar-4%H_2-2%H_2O. The TGO-thickness at failure could not be accurately measured since the oxide completely spalled off together with the ceramic topcoat, as it is frequently found for EB-PVD TBC-coatings. Therefore, the available TGO-thickness data after oxidation in both atmospheres were extrapolated to estimate the TGO-thickness at failure assuming the common power law time dependence for the thickening rate (Fig. 14c). The data show that the estimated TGO-thickness at TBC-failure is ca. 6 μm for both atmospheres, which is apparently the critical TGO-thickness for the studied EB-PVD TBC-system under the used temperature cycling conditions.

It should be noted that the TGO-microstructure shown in Fig. 13 is typical for MCrAlY-alloys and coatings with a low Y-content, typically 0.2 wt%. At higher Y-contents and with additions of other REs such as Zr and Hf the TGO-microstructure may substantially deviate from the ideal columnar morphology shown in Fig. 13. This change is the result of incorporation of the internal precipitates of the RE-oxides into the alumina scale. The effect was

illustrated first on FeCrAlY-alloys with additions of Zr [15]. The implications of minor Hf, Zr additions to the MCrAlY-coatings for the lifetime of the TBCs are discussed elsewhere in the present article (see the sections "Failure of EB-PVD-TBC's on MCrAlY-bondcoats" and "Effect of process environment during plasma spraying").

Effect of manufacturing related parameters on MCrAlY-oxidation behavior and TBC-lifetime

General remarks

Even if the same MCrAlY-powder and the same spraying parameters for bondcoat deposition are used prior to the manufacturing of EB-PVD and APS-TBCs the TGO-formation can be different between the two TBC-systems. These differences mainly arise from differences in the manufacturing steps after the bondcoat deposition. For APS-TBCs the bondcoat is subjected to a densification vacuum heat-treatment followed directly by the top-coat deposition. For EB-PVD TBCs the bondcoat is, after the vacuum heat-treatment subjected to a surface smoothening treatment, thereby reducing the bondcoat roughness and removing the changes in surface chemical composition and microstructure introduced by the vacuum heat-treatment.

The bondcoat deposition can be performed by a variety of methods, including APS, Ar-shrouded plasma spraying, VPS, high velocity oxyfuel (HVOF). Each process is characterized by a number of parameters such as

temperature/velocity of particles as well as process environment (air, Ar, vacuum) in plasma spraying methods and vacuum quality and deposition rate in EB-PVD. In turn, the densification heat-treatment can be performed in vacuum or inert gas and the temperature regime may differ depending on the superalloy composition. The bondcoat smoothening prior to EB-PVD-TBC deposition can be performed by grinding or barrel (media) finishing, followed by grit blasting and/or shot-peening.

Yanar et al. [40] described a significant effect of the pre-treatment procedures on the EB-PVD-TBC-lifetime. Very smooth bondcoat surfaces provided the longest lifetime, but the lifetime reproducibility was worse compared to the bondcoats with moderate surface roughness. This was attributed to the lower number of nucleation sites for defects but easier crack propagation on very smooth surfaces. One important outcome of this study was that the pre-treatment procedure commonly used in industrial applications is in many cases not optimized for achieving extended and reproducible TBC-lifetimes.

Therefore, in the following section the effect of the bondcoat geometrical parameters (roughness and thickness) and that of the oxygen content during spraying on the RE-distribution in the coating and TGO-formation will be discussed in more detail.

Effect of MCrAlY-coating geometrical parameters on TGO-morphology and TBC-lifetime

The deposition by plasma spraying results intrinsically in a rough coating surface. Typical Ra (arithmetic mean

roughness) values reported in literature vary between 4–5 and 10–15 μm. It is important to mention that the Ra parameter does not accurately describe the surface morphology and coatings with very similar Ra values can exhibit quite different roughness profiles. The latter depend on a number of factors such as particle size distribution in the powder, deposition method (APS, VPS, or HVOF) and detailed spraying parameters.

Recently it has been shown [41] that oxidation of rough MCrAlY-surfaces intrinsically results in the formation of an inhomogeneous TGO. In the concave coating regions the TGO contains significant amounts of Y-aluminate pegs, resulting in locally accelerated TGO-growth rate. In the convex regions, the TGO consisted mainly of pure alumina occasionally covered with $NiCr_2O_4$ nodules. These observations were related to a faster depletion of Y and Al underneath the convex regions of the coating compared to the concave regions. On flat (ground) surfaces of the same coating the scale morphology and distribution of Y-aluminate pegs was uniform (Fig. 15). Obviously, the exact distribution of the Y-oxide pegs induced by the coating surface geometry depends on the coating roughness profile, Y and Al-content as well as service temperature. The inhomogeneous distribution of Y-aluminate pegs is not an intrinsic feature of rough surfaces in the APS-TBC-systems but can be found also in the EB-PVD-TBC-systems, depending on the extent of surface smoothening (Fig. 16). The inhomogeneous scale formation is one of the reasons why it is difficult to define a critical TGO-thickness for failure in the APS-TBC-systems, as discussed in the

Fig. 15 SEM-BSE images of cross-sections of a 1.5 mm thick, free-standing VPS NiCoCrAl-0.5%Y-coating after 25 h isothermal oxidation at 1,100 °C in air: a rough, as-sprayed surface and b ground surface
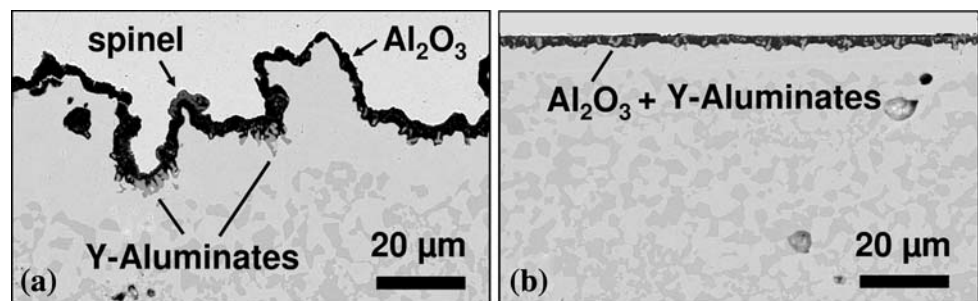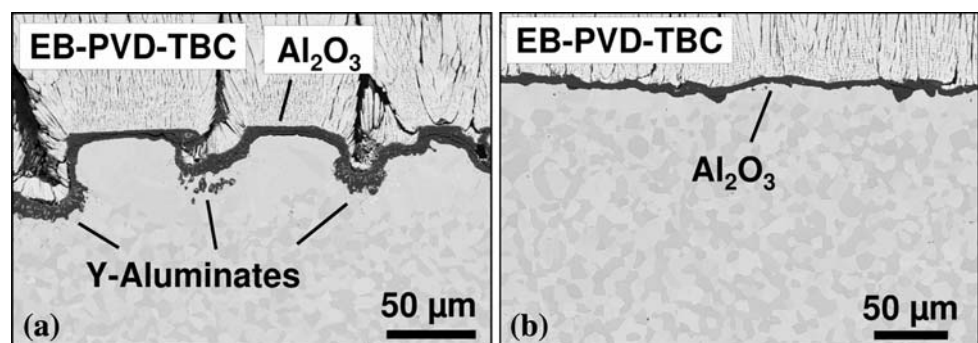

Fig. 16 SEM-BSE images of cross-sections of an EB-PVD-TBC-system on conventionally cast Ni-base superalloy with VPS NiCoCrAlY-bondcoat after long-term cyclic oxidation at 1,000 °C in air: partial a and extensive b smoothening prior to TBC-deposition during manufacturing

section "Failure mechanisms of APS-TBC's on MCrAlY-bondcoats" above.

In spite of the fact that typically in EB-PVD-TBC-systems the smoothening results in a relatively flat TBC/BC interface such as that shown in Fig. 16b, variations in the TGO-morphology and growth rate in nominally the same systems can be observed depending on the bondcoat thickness as shown recently in reference [42]. The effect could be unequivocally demonstrated on a free-standing, VPS CoNiCrAlY-coating from which specimens of different thickness were oxidized at 1,100 °C. During oxidation, thicker specimens exhibited higher scale growth rates than thinner specimens. The increase of the TGO-growth rate on the thick specimens was attributed to a larger Y-reservoir resulting in more extensive internal oxidation of Y and incorporation of Y-aluminate pegs into the TGO (Fig. 17). Recently a model was developed [43] to predict the amount of Y-oxide pegs formed in the TGO and the associated Y-depletion in the coating during oxidation.

By affecting the Y-reservoir, bondcoat thickness affects the TGO-growth rate as well as adherence. Consequently, variations in the bondcoat thickness should also have an effect on the TBC-lifetime. Figure 18 shows the lifetime data of two EB-PVD-TBC-systems with two different bondcoat thicknesses. The short time to TBC-failure with a thinner (60 μm) bondcoat can be explained by a smaller Y-reservoir and consequently poorer TGO-adherence as compared to "standard", 200 μm bondcoat. The results of the free-standing coatings (Fig. 17), however, indicate that increasing the coating thickness also results in a higher TGO-growth rate. Therefore, in very thick bondcoats the positive effect of improving the TGO-adherence by increasing the Y-reservoir can be overcompensated by the negative TGO-"overdoping" [11], thereby shortening the
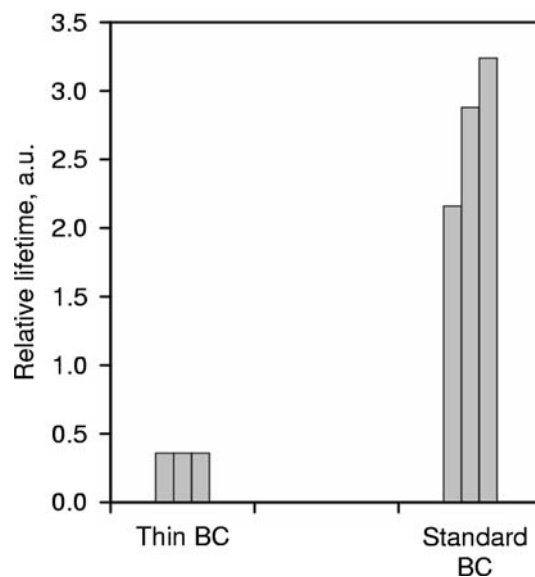

Fig. 18 Relative lifetime of EB-PVD-TBC-systems during cyclic oxidation (2 h heating/15 min cooling) at 1,100 °C in air with 60 μm "Thin" NiCoCrAlY-bondcoat and 200 μm "Standard" bondcoat

time to reach the critical TGO-thickness for TBC-failure. These opposite effects imply that for a given TBC-system there should exist an optimum coating thickness (Y-reservoir) providing the longest TBC-lifetime [42].

Effect of process environment during plasma spraying

During manufacturing the MCrAlY-coating material is in contact with various oxidizing media at high temperatures. This occurs during the powder gas-atomization, the thermal spraying as well as during the heat-treatment and TBC-deposition, whereby uptake of impurities (oxygen in the first place) can be significant even during the densification

Fig. 17 Effect of specimen thickness on oxidation rate of free-standing VPS NiCoCrAlY-coating with 0.6%Y during discontinuous air oxidation at 1,100 °C: **a** Mass change data; **b**, **c** SEM-BSE images of cross-sections after 110 h exposure of 0.15 mm and 2 mm specimens, respectively
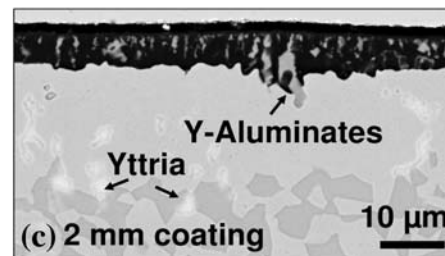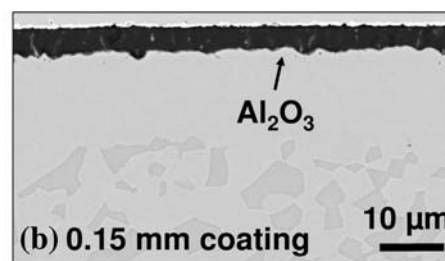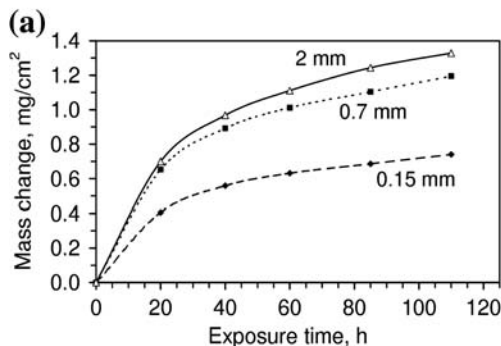
vacuum heat-treatment. An extreme case is the oxidation of MCrAlY-powder particles in the cost-attractive APS bondcoat deposition process, whereby such coatings were shown to generally exhibit poor oxidation resistance [5]. The latter was related to the alumina layers formed during spraying at the coating splat boundaries, which allowed oxygen ingress and hindered Al-diffusion from the bulk bondcoat to the surface during subsequent oxidation. This "diffusion cell effect" resulted in a premature failure of the coating due to formation of voluminous spinel-type oxides. This effect is generally not observed in the case of MCrAlY-coatings deposited by vacuum plasma spraying due to much lower oxygen content in the spraying environment. However, in the latter case yttrium was found to oxidize thereby forming fine precipitates in a VPS overlay coating [44]. More recently, high residual oxygen content within the vacuum chamber has been shown [14] to result in tying up the REs (Y and Hf) into oxides within the bondcoat of a TBC-system. During subsequent cyclic oxidation testing of this system, the TGO consisted of almost pure alumina, however, the lifetime of the TBCs was extremely short (Fig. 19a). In contrast, the bondcoat with a low oxygen content (sprayed under high vacuum) formed a non-homogeneous TGO containing fine Y and Hf-oxide precipitates. This TGO exhibited a higher growth rate, but the TBC-lifetime was much longer than in the case of the "high-oxygen" MCrAlY-coating (Fig. 19b). The latter observation is qualitatively similar to that made on the TBC-system with the MCrAlY, Zr-containing bondcoat (compare Fig. 19b and Fig. 3). It is related to development of an uneven TGO/BC interface, whereas the failure occurs at the TBC/TGO-interface. The effect of the vacuum quality (residual oxygen content) during VPS on the TGO-morphology and growth rate was verified by spraying of free-standing coatings under intentionally varied vacuum conditions [14].

The results presented in this section indicate that the positive effect of MCrAlY-bondcoat co-doping with Hf and Zr on the TGO-morphology and associated TBC-lifetime can be suppressed if the REs are tied up in oxide phases during spraying. On the other hand excessive Zr

(Hf) incorporation into the scale might shorten the TBC-lifetime due to scale "overdoping" resulting in excessively high scale growth rates. Therefore, the major challenge for the TBC-lifetime extension by formation of an uneven TGO/BC interface is to define and reproduce an optimal Zr (Hf) reservoir in the coating, which depends on a number of parameters such as Zr (Hf) content, amount of O and C impurities and coating thickness.

One of the ways to modify the Hf/Zr-distribution in the MCrAlY-coatings prior to the oxidation exposure is the vacuum heat-treatment of the bondcoat. This is discussed in detail in the next section.

Effect of heat-treatment parameters on RE-distribution and TGO-growth

General remarks

After deposition the bondcoat is commonly subjected to a vacuum heat-treatment. One of the effects observed during vacuum heat-treatment is Cr-evaporation, which results in an enrichment of the β-NiAl-phase at the MCrAlY-bondcoat surface [12]. Furthermore, the heat-treatment affects the distribution of the REs in the coating. Several authors observed formation of Y-rich oxides on the coating surface and/or in the sub-surface regions after the vacuum heat-treatment [45, 46]. In reference [12] EB-PVD MCrAlY-bondcoats were heat-treated at different residual vacuum pressures at 1,100 °C prior to the TBC-deposition. During subsequent air oxidation the longest TBC-lifetime was obtained for specimens which had been subjected to a two-stage heat-treatment, i.e., short-term heating in high vacuum followed by a 2–4 h anneal in low vacuum of about 100 Pa. In this way, a thin alpha alumina-based scale with a high density of Y-rich oxide pegs formed during the subsequent air oxidation, resulting in superior TBC-lifetime compared to the coatings which had been subjected to a standard industrial heat-treatment procedure. A positive effect of the heat-treatment of an MCrAlY-bondcoat prior to

Fig. 19 EB-PVD-TBC-specimens with MCrAlYHf-bondcoat after cyclic oxidation (2 h cycles) to macroscopic TBC-failure at 1,000 °C: a Realtive Lifetime of 6.5, high O-content in bondcoat; b Relative lifetime of 49, low O-content in bondcoat
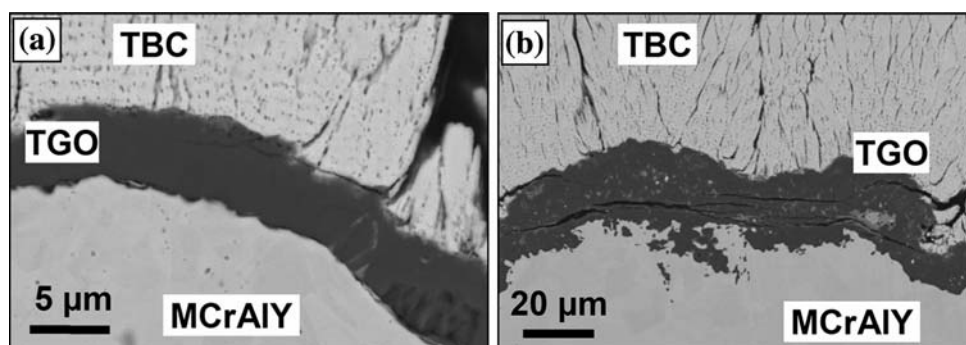
TBC-deposition in vacuum compared to that in Ar-H$_2$ on the TBC-lifetime was found in [47].

The heat-treatment procedure used in practice is optimized for obtaining the desired microstructure and consequently high creep strength of the substrate superalloy. For instance, for conventionally cast superalloys such as Inconel 738 a solution annealing step of 2 h at 1,120 °C is followed by γ'-Ni$_3$Al-precipitation for 24 h at 845 °C [48]. However, a different heat-treatment procedure can be applied if the same MCrAlY-coating is deposited on other (types of) superalloys. For example for single crystal superalloy Rene N4 the procedure is [48] 2 h at 1,270 °C + 4 h at 1,080 °C + 16 h at 900 °C. Considering the results in [45, 46] this means that for a given bondcoat the RE distribution established during manufacturing can vary between TBC-systems on different superalloys.

In the sections "Failure of EB-PVD-TBC's on MCrAlY-bondcoats" and "Effect of process environment during plasma spraying", the incorporation of minor RE additions, Hf and Zr from the MCrAlY-Hf(Zr)-bondcoat into the TGO was shown to modify substantially the TGO-morphology thereby extending the TBC-lifetime. Considering the high affinity of Hf and Zr to oxygen it is likely that their distributions can be affected by the vacuum heat-treatment in a similar manner as Y possibly with consequences for the TGO-growth rate and adhesion.

In the following section the Y and Hf distributions in a MCrAlYHf-coating after two different heat-treatment procedures are studied using a range of analytical techniques. Hence, the determined RE-distributions are correlated with the TGO-morphologies formed during oxidation of the heat-treated samples. In order to separate possible effects of superalloy and/or TBC on TGO-growth this work was carried out using free-standing coatings. Subsequently, possible implications of the presented results for the lifetime of TBC-systems are discussed.

Y and Hf distribution after vacuum heat-treatment

Vacuum heat-treatment at 10^{-5} mbar base pressure performed at 1,100 °C for 2 h resulted in the formation of Y and Hf-rich oxides on the coating surface (Fig. 20a). The

internal oxidation zone (about 15 μm) consisted mainly of coarse yttria precipitates (Fig. 21a, c). No alumina formation was detected by a range of analytical techniques including laser-induced fluorescence spectroscopy, SNMS and SEM. This seems, at first sight, to be surprising considering the fact that the residual oxygen partial pressure prevailing in the vacuum chamber (vacuum of 10^{-5} mbar) is substantially larger than the dissociation pressure of alumina (10^{-26} bar). However, according to Hertz-Langmuir equation, the oxygen impingement rate under the vacuum of 10^{-5} mbar is extremely low (eight orders of magnitude lower than that in air). Therefore the Y flux from the bulk coating to the surface was sufficiently high to tie up all oxygen transferred to the coating surface into Y-oxide thereby reducing the oxygen activity at the coating surface below the dissociation pressure of alumina [14]. SNMS-depth profiles of the heat-treated specimens showed that the Y-oxide formation at the surface results in substantial Y-depletion within the coating.

After vacuum heat-treatment at lower temperatures, such as at 1,000 °C for 24 h, however, the surface oxide precipitates mainly consisted of hafnia and alumina, whereas the yttrium formed a wide internal oxidation zone of fine oxide precipitates (Figs. 20b and 21b, d). The latter observations can be explained by a reduced mobility of yttrium at 1,000 °C, with the result that the oxygen partial pressure established at the coating surface was sufficiently high to form the alumina precipitates. Furthermore due to the reduced mobility of yttrium at 1,000 °C nucleation of internal yttria precipitates in the coating matrix was promoted rather than their growth. This explains the extended width of the internal oxidation zone and finer precipitate size for yttria compared to that formed at 1,100 °C. It is important to mention that the Y/Hf-oxide formation during vacuum heat-treatment results in depletion of these elements from the coating.

On rough surfaces of the studied Hf-containing NiCoCrAlY-bondcoat after vacuum annealing a similar temperature dependence of the RE-oxide type and distribution was observed (Fig. 22). The formation of alumina at 1,000 °C was, however, localized at the bondcoat hills, whereas in the valleys formation of Hf and Y-rich oxides

Fig. 20 SNMS-depth profiles of 1.5 mm free-standing flat NiCoCrAlY + Hf coating after vacuum heat-treatment at 10^{-5} mbar: a for 2 h at 1,100 °C and b for 24 h at 1,000 °C
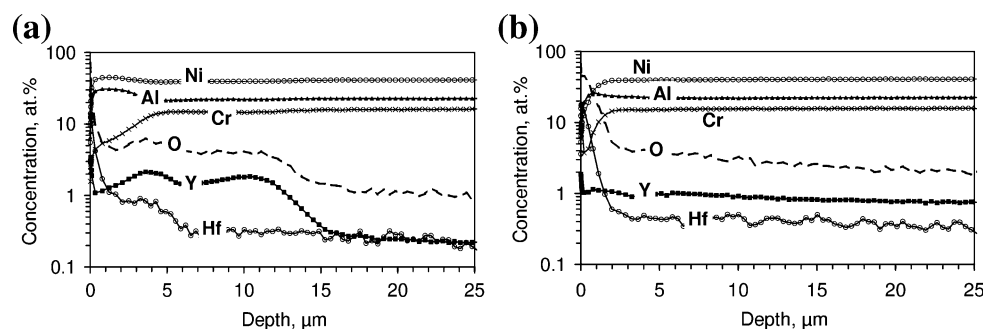
Fig. 21 SEM cross-sections of 1.5 mm NiCoCrAlY + Hf free-standing coatings (flat surfaces) after vacuum heat-treatment at 10^{-5} mbar for 2 h at 1,100 °C (**a, c**) and 24 h at 1,000 °C (**b, d**). **a, b** backscattered electron images and **c, d** panchromatic cathodoluminescence images
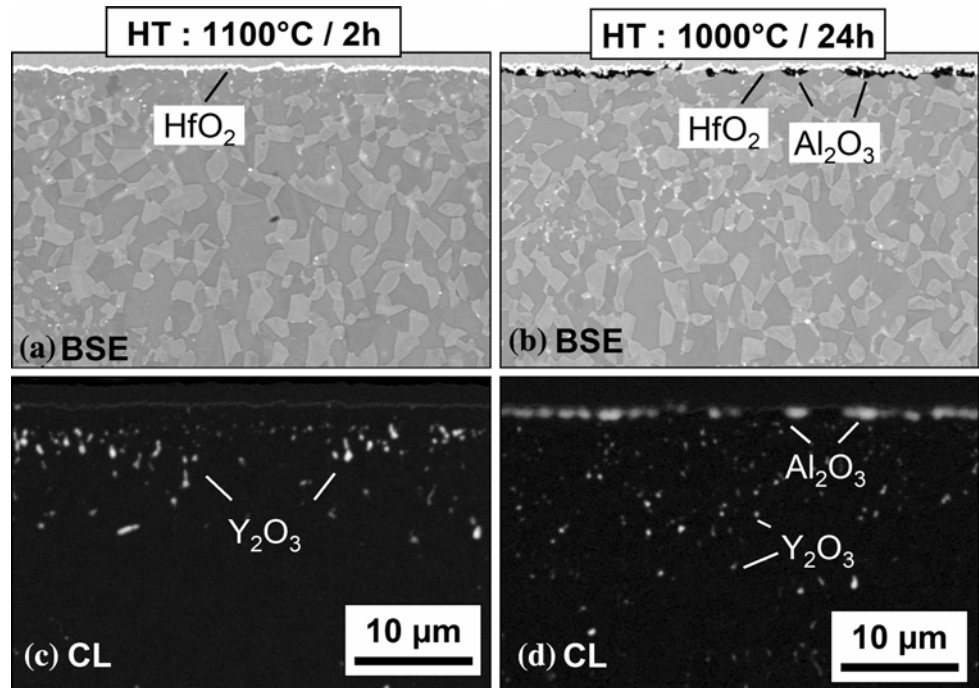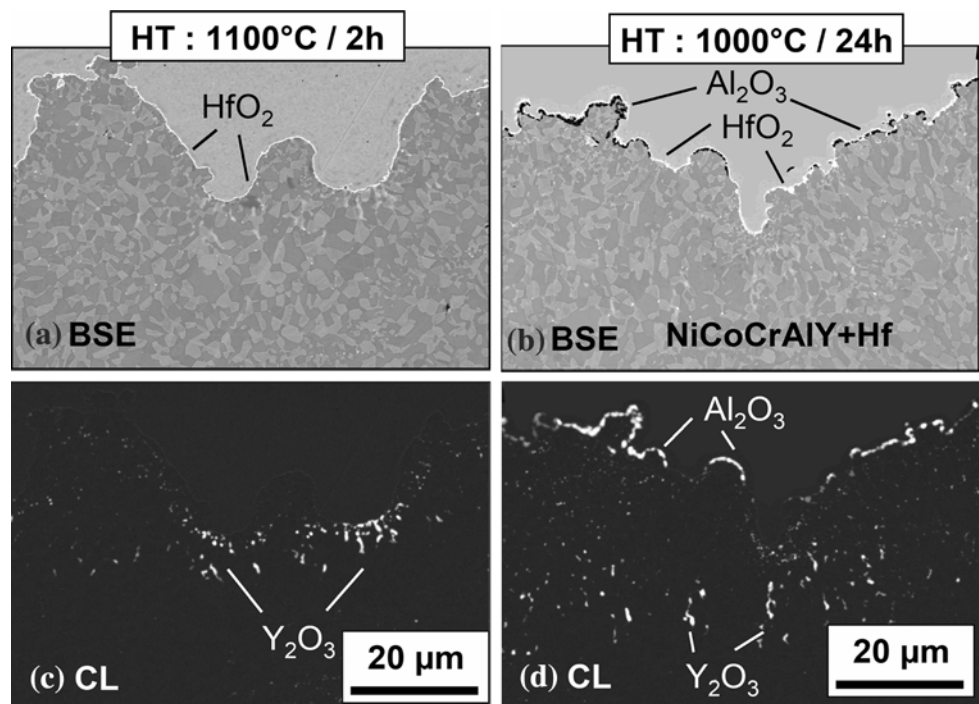

Fig. 22 SEM cross-sections of 1.5 mm NiCoCrAlY + Hf free-standing coatings (rough sprayed surface) after vacuum heat-treatment at 10^{-5} mbar for 2 h at 1,100 °C (**a, c**) and 24 h at 1,000 °C (**b, d**). **a, b** backscattered electron images and **c, d** panchromatic cathodoluminescence images

occurred. This can be explained by the non-uniform RE-depletion underneath the rough surfaces. Comparing these observations with those made in oxidized, Y-doped MCrAlY described in the section "Effect of MCrAlY-coating geometrical parameters on TGO-morphology and TBC-lifetime". Figure 15 reveals that the inhomogeneous RE-distribution occurs already during vacuum heat-treatment, i.e., prior to the actual oxidation exposure in service.

Effect of Y and Hf distribution established by heat-treatment on TGO-morphology

The RE-oxide distribution established during vacuum heat-treatment affects the oxide scale growth rate and morphology during subsequent air oxidation at 1,100 °C (Fig. 23). The coating heat-treated for 2 h at 1,100 °C showed a stronger tendency to inward scale growth and a
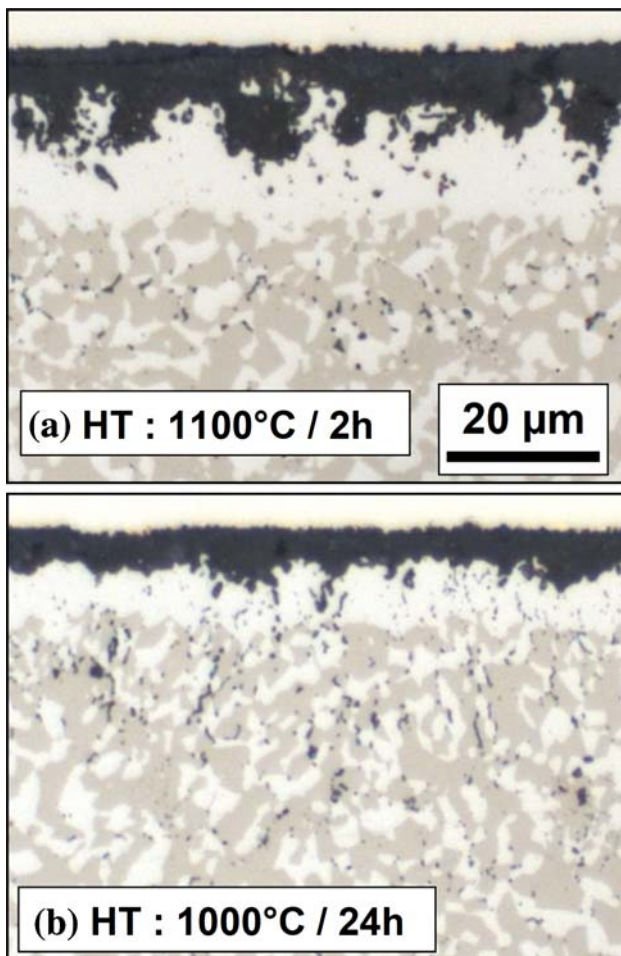
Fig. 23 Optical metallographic cross-sections of 0.2 mm thick, free-standing NiCoCrAlY + Hf coatings after 72 h isothermal oxidation at 1,000 °C in air showing effect of preceding vacuum heat-treatment on oxide scale formation: **a** heat-treated for 2 h at 1,100 °C and **b** heat-treated for 24 h at 1,000 °C (vacuum of 10^{-5} mbar)

deeper penetration of oxide intrusions. This is related to the Y/Hf-oxides formed during heat-treatment in the near-surface regions, which act as short-circuit paths for oxygen transport during the subsequent air oxidation. In contrast, the coating heat-treated for 24 h at 1,000 °C exhibited a lower scale growth rate and less oxide intrusions than the material heat-treated at 1,100 °C for 2 h (Fig. 23). This effect can be attributed to partly tying up yttrium/hafnium as oxide precipitates deep in the coating by the lower temperature, long time heat-treatment, thereby reducing scale overdoping during subsequent oxidation as a result of excessive incorporation of Y/Hf into the alumina scale.

The results in this section demonstrate that the temperature regime of the vacuum heat-treatment has a significant influence on the TGO-growth rate on the MCrAlY-bondcoats, especially if these are co-doped with Hf and/or Zr. High heat-treatment temperature under high vacuum promotes RE-oxidation at the coating surface and

consequently enhances the TGO-growth rate during oxidation. In the section "TGO-growth rate and its effect on TBC-lifetime" above it was shown that the TBC-failure occurs at a critical TGO-thickness. Therefore, by affecting the TGO-growth rate, the heat-treatment parameters (temperature, time, and perhaps also vacuum quality) should have an effect on the TBC-lifetime. Additional studies are required to verify the extent of this effect in "real" TBC-systems.

One of the means to prevent the negative effects of RE-oxide formation at the surface on the TGO-formation can be tying up Y (Zr, Hf) into stable, homogeneously distributed compounds prior to heat-treatment. This could be done, e.g., by introducing the REs into the powder as oxide dispersion. Ajdelsztajn et al. [49] produced yttrium ODS MCrAlY-powder by cryomilling. After VPS-spraying this powder into a coating, a homogeneous Y-distribution in the bondcoat in form of fine yttria particles (20–50 nm size/ 500 nm distance) was obtained. The lifetime of the APS-TBC on the ODS-bondcoat was claimed to be a factor of three longer compared to the bondcoat sprayed from the conventional, non-cryomilled powder. The authors attributed the TBC-lifetime extension by powder cryomilling to an improved creep strength and a reduction in CTE of the bondcoat. However, based on the considerations in the previous sections it seems likely that the fine distribution of the yttria dispersions also resulted in an improved adherence of the TGO especially in the bondcoat hills. This effect of improved scale adherence by RE-oxide dispersion can be similar to the observations made previously with bulk alumina forming ODS materials [34]. It should be noted that in order to get such an ODS-effect a very uniform distribution of fine RE-oxide dispersion is required. Typical optimized yttria dispersions in ODS alloys are about 20 nm in size and an interparticle distance is less than 150 nm [50]. These values are comparable with those achieved during cryomilling powder processing in [49]. In contrast, if the Y is oxidized during processing but is not homogeneously distributed its positive effect on the scale adherence can be lost, as was apparently the case of the bondcoats sprayed under poor vacuum conditions (see the section "Effect of process environment during plasma spraying").

Concluding remarks

The oxidation behavior of MCrAlY-bondcoat plays a decisive role for the lifetime of TBCs.

At T ≤ 1,000 °C the phase compositions of MCrAlY-coatings with a low Co-content (≤ 20 wt%) do not solely consist of $\gamma+\beta$. This is a result of phase transformations, such as $\gamma+\beta\rightarrow\gamma'+\alpha(\sigma)$ upon cooling from 1,050 to 1,100 °C.

These transformations are associated with a volume change resulting in an increase of the coating CTE. Consequently the TGO-adherence is deteriorated and TBC-lifetime is shortened compared to Co-rich MCrAlY-coatings.

For EB-PVD-TBC-systems the formation of flat, uniform alumina scales consisting of pure alumina is frequently an indication of a small Y-reservoir in the bondcoat. Such scale morphology facilitates the crack propagation commonly initiated at the TGO/BC interface during cyclic oxidation and, therefore, might not be optimal for an extended TBC-lifetime. In contrast, formation of heterogeneous, inwardly growing alumina scales by minor additions of Zr (Hf) to the MCrAlY-coating shifts the crack initiation/propagation sites from the TGO/BC toward the TGO/TBC interface resulting in TBC-lifetime extension. The non-uniform scale morphology is, however, associated with an accelerated scale growth rate. Furthermore it is very sensitive to the coating manufacturing parameters, which to a large extent determines the reservoir of the RE, such as Y, Zr, and Hf. The manufacturing parameters of importance are: vacuum quality during spraying (tying up RE in oxides), vacuum and temperature parameters during heat-treatment (RE-oxide formation at the coating surface, RE-depletion from the coating), smoothening (removal of surface RE-oxides formed during heat-treatment). By varying the thickness of free-standing NiCoCrAlY-coatings and bondcoat in a TBC-system it could be demonstrated that the TGO-growth rate and adherence are affected not only by the RE-content but also by the RE-reservoir, and thus by the coating thickness. The RE-oxides formed during vacuum heat-treatment on the coating surface affect the growth rate of the TGO. By oxidation in controlled atmospheres with different oxygen partial pressures it could be unequivocally shown that, for a specific EB-PVD-TBC-system forming flat, uniform alumina TGO and under given testing condition the TBC-failure occurs after reaching a critical TGO-thickness.

In APS-TBC-systems the rough bondcoat surface results in formation of intrinsically heterogeneous TGOs. This is related to an inhomogeneous RE/Al-depletion beneath the rough surfaces. The TBC-failure seems to be initiated by crack formation at the TGO/BC interface on the "hills" of the rough coating surface, which occurs already at relatively short exposure times. Repeated-cracking and inhomogeneous TGO-formation on rough surfaces of many APS-TBC-systems make difficult or impossible definition of a critical TGO-thickness for failure. The crack propagation and time to APS-TBC-failure are largely governed by the mechanical properties and microstructure of the TBC. Optimization of these properties as well as the bondcoat roughness by manufacturing, therefore, offers a potential for lifetime extension and improvement of lifetime reproducibility of APS-TBC-coatings.

References

1. Goward GW (1998) Surf Coat Technol 108–109(1–3):73
2. Gleeson B (2006) J Propul Power 22–2:375
3. Evans AG, Mumm DR, Hutchinson JW, Meier GH, Pettit FS (2001) Prog Mater Sci 46:505
4. Quadakkers WJ, Tyagi AK, Clemens D, Anton R, Singheiser L (1999) In: Hampikian JM, Dahotre NB (eds) Elevated temperature coatings: surface and technology III. The Minerals, Metals & Materials Society, pp 119–130
5. Niranatlumpong P, Ponton CB, Evans HE (2000) Oxid Met 53(3–4):241
6. Busso EP, Wright L, Evans HE et al (2007) Acta Mater 55:1491
7. Tolpygo VK, Clarke DR, Murphy KS (2001) Surf Coat Technol 146–147:124
8. Evans HE, Strawbridge A, Carolan RA, Ponton CB (1997) Mater Sci Eng A 225:1
9. Quadakkers WJ, Shemet V, Sebold D, Anton R, Wessel E, Singheiser L (2005) Surf Coat Technol 199(1):77
10. Janakiraman R, Meier GH, Pettit FS (1999) Metall Mater Trans A 30:2905
11. Pint BA (2003) J Amer Ceram Soc 86(4):686
12. Nijdam TJ, Marijnissen GH, Vergeldt E, Kloosterman AB, Sloof WG (2006) Oxid Met 66:269
13. Schulz U, Menzebach M, Leyens C, Yang YQ (2001) Surf Coat Technol 146–147(5/6):117
14. Subanovic M, Sebold D, Vassen R, Wessel E, Naumenko D, Singheiser L, Quadakkers WJ (2008) Mater Corros 59(6):463
15. Wessel E, Kochubey V, Naumenko D, Niewolak L, Singheiser L, Quadakkers WJ (2004) Scripta Mater 51(10):987
16. Mercer C, Faulhaber S, Yao N, McIlwrath K, Fabrichnaya O (2006) Surf Coat Technol 201:1495
17. Evans AG, Crumley GB, Demaray RE (1983) Oxid Met 20(5/6): 193
18. Naumenko D, Gleeson B, Wessel E, Singheiser L, Quadakkers WJ (2007) Metall Mater Trans 38A:2974
19. Hsueh CH, Haynes JA, Lance MJ et al (1999) J Amer Ceram Soc 82(4):1073
20. Tang F, Schoenung J (2005) Scripta Mater 52:905
21. Ahrens M, Vaßen R, Stoever D (2002) Surf Coat Technol 161:26
22. Trunova O, Beck T, Herzog R, Steinbrech RW, Singheiser L (2008) Surf Coat Technol 202:5027
23. Fox P, Tatlock GJ (1989) Mater Sci Technol 5:816
24. Czech N, Schmitz F, Stamm W (1994) Surf Coat Technol 68–69:17
25. Massalski TB (1996) ASM binary alloy phase diagrams. ASM International, Materials Park, OH
26. Achar DRG, Munoz-Arroyo R, Singheiser L, Quadakkers WJ (2004) Surf Coat Technol 187:272
27. Muñoz-Arroyo R, Clemens D, Tietz F, Anton R, Quadakkers J, Singheiser L (2001) Mater Sci Forum 369–372:165

28. Täck U (2004) The influence of cobalt and rhenium on the behaviour of MCrAlY coatings (PhD thesis) Tech. Univ. Freiberg 25:151, 169

29. Toscano J, Gil A, Hüttel T, Wessel E, Naumenko D, Singheiser L, Quadakkers WJ (2007) Surf Coat Technol 202:603

30. Lechner C, Seume J (eds) (2003) Stationaere Gasturbinen. Springer-Verlag, Berlin Heidelberg, Germany, p 749

31. Jansson B, Schalin M, Selleby M, Sundaman B (1993) In: Bale CW, Irins GA (eds) Computer software in chemical and extractive metallurgy. Canadian Institute of Metals, Quebec, p 57

32. Saunders N (2000) Ni-DATA information. Thermotech Ltd., Surrey Technology Centre, Surrey, UK

33. Echsler H, Renusch D, Schütze M (2004) Mater Sci Technol 20:307

34. Quadakkers WJ, Holzbrecher H, Briefs KG, Beske H (1989) Oxid Met 32(12):67

35. Pint BA, Martin JR, Hobbs LW (1993) Oxid Met 39:167

36. Reddy KPR, Smialek JL, Cooper AR (1982) Oxid Met 17(5/6):429

37. Karadge M, Zhao X, Preuss M, Xiao P (2006) Scripta Mater 54:639

38. Toscano J, Wessel E, Vassen R, Naumenko D, Singheiser L, Quadakkers WJ (2008) Mater Corros 59(6):501

39. Kofstad P (1988) High temperature corrosion. Elsevier, London

40. Yanar NM, Pettit FS, Meier GH (2006) Metall Mater Trans 37A:1563

41. Gil A, Shemet V, Vassen R, Subanovic M, Toscano J, Naumenko D, Singheiser L, Quadakkers WJ (2006) Surf Coat Technol 201:3824

42. Toscano J, Vaßen R, Gil A, Subanovic M, Naumenko D, Singheiser L, Quadakkers WJ (2006) Surf Coat Technol 201:3906

43. Nijdam TJ, Sloof WG (2008) Oxid Met 69:1

44. Gudmundsson B, Jacobson BE (1989) Thin Solid Films 173(1):99

45. Nijdam TJ, Jeurgens LPH, Chen JH, Sloof WG (2005) Oxid Met 64(5/6):355

46. Schulz U, Bernardi O, Ebach-Stahl A et al (2008) Surf Coat Technol 203:160

47. Lau H, Leyens C, Schulz U, Friedrich C (2003) Surf Coat Technol 165:217

48. Davis JR (ed) (1997) Heat resistant materials, ASM specialty handbook. ASM International, Materials Park, OH, p 305

49. Ajdelsztajn L, Hulbert D, Mukherjeea A, Schoenung JM (2007) Surf Coat Technol 201:9462

50. Wasilkowska A, Bartsch M, Messerschmidt U et al (2003) J Mater Process Technol 133:218